



## New constraints on the timing of sea level fluctuations during early to middle marine isotope stage 3

E. J. Rohling,<sup>1</sup> K. Grant,<sup>1</sup> C. Hemleben,<sup>2</sup> M. Kucera,<sup>2</sup> A. P. Roberts,<sup>1</sup> I. Schmeltzer,<sup>2</sup>  
H. Schulz,<sup>2</sup> M. Siccha,<sup>2</sup> M. Siddall,<sup>3</sup> and G. Trommer<sup>2</sup>

Received 1 March 2008; revised 17 June 2008; accepted 1 July 2008; published 17 September 2008.

[1] To settle debate on the timing of sea level fluctuations during marine isotope stage (MIS) 3, we present records of  $\delta^{18}\text{O}_{\text{ruber}}$  (sea level proxy) and magnetic susceptibility from the same samples within the single sediment archive (i.e., “coregistered”) of central Red Sea core GeoTü-KL11. Core-scanning X-ray fluorescence and environmental magnetic data establish the suitability of magnetic susceptibility as a proxy for eolian dust content in Red Sea sediments. The eolian dust data record similar variability as Greenland  $\delta^{18}\text{O}_{\text{ice}}$  during early to middle MIS 3, in agreement with previous observations that regional Arabian Sea climate fluctuated with a timing similar to that of Greenland climate variations. In contrast, the sea level record fluctuates with a timing similar to that of Antarctic-style climate variations. The coregistered nature of the two records in core KL11 unambiguously reveals a distinct offset in the phase relationship between sea level and eolian dust fluctuations. The results confirm that sea level rises, indicated by shifts in Red Sea  $\delta^{18}\text{O}_{\text{ruber}}$  to lighter values, occurred during cold episodes in Greenland during early to middle MIS 3. This indicates that the amplitudes of the reconstructed MIS 3 sea level fluctuations would not be reduced by inclusion of regional climate fluctuations in the Red Sea sea level method. Our analysis comprehensively supports our earlier conclusions of large-amplitude sea level variations during MIS 3 with a timing that is strongly similar to Antarctic-style climate variations.

**Citation:** Rohling, E. J., K. Grant, C. Hemleben, M. Kucera, A. P. Roberts, I. Schmeltzer, H. Schulz, M. Siccha, M. Siddall, and G. Trommer (2008), New constraints on the timing of sea level fluctuations during early to middle marine isotope stage 3, *Paleoceanography*, 23, PA3219, doi:10.1029/2008PA001617.

### 1. Introduction

[2] There is considerable debate about the timing of sea level fluctuations during marine isotope stage (MIS) 3 relative to other key signals of climate variability during that period from Greenland and Antarctic ice core records. This is an important debate, because it has the potential to provide observational constraints to the question whether global ice volume would increase during relatively warm or relatively cold periods in the Greenland climate record, and hence will inform our developing understanding (and modeling) of the underlying processes.

[3] We previously proposed that sea level variability closely followed an Antarctic-style rhythm of climate variability [Siddall *et al.*, 2003; Rohling *et al.*, 2004], based on a comparison of signal structure in a central Red Sea sea level record with that in ice core climate records during MIS 3. This assertion is supported by strong signal similarity that had been noted between deep-sea benthic foraminiferal  $\delta^{18}\text{O}$  records and Antarctic climate variability [Shackleton *et al.*, 2000; Cutler *et al.*, 2003; Pahnke *et al.*, 2003; Pahnke and Zahn, 2005]. This Antarctic-style

signal structure is so ubiquitous in benthic foraminiferal  $\delta^{18}\text{O}$  records that it remains recognizable even in a statistical stack of 57 individual records [Lisiecki and Raymo, 2005; Siddall *et al.*, 2008b]. However, benthic  $\delta^{18}\text{O}$  records may be affected by deep-sea temperature fluctuations and changes in advection and mixing of different source waters, so this signal structure comparison does not conclusively validate our synchronization.

[4] Recently, Arz *et al.* [2007] described an empirically calibrated sea level record from the northern Red Sea, which has similar structure to the model-interpreted version from the central Red Sea of Siddall *et al.* [2003] (see comparison by Siddall *et al.* [2008a]). However, Arz *et al.* [2007] proposed an alternative synchronization to the ice core records for a northern Red Sea sediment core, based on a range of AMS  $^{14}\text{C}$  datings of foraminiferal calcite, and age tie points from geomagnetic paleointensity variations. The paleointensity minimum associated with the Laschamp geomagnetic excursion was used as a globally isochronous marker for Dansgaard-Oeschger interstadial 10 based on correlation with cosmogenic  $^{10}\text{Be}$  data from Greenland ice cores [Muscheler *et al.*, 2005]. Theoretically, this would establish the phasing of the sea level driven Red Sea record relative to the Greenland ice core temperature signal. Although the amplitudes in the sea level record of Arz *et al.* [2007] generally agree with those of Siddall *et al.* [2003] (see comparison by Siddall *et al.* [2008a]), Arz *et al.* [2007] thus inferred that sea level rises coincided with warming in the Greenland records, which would imply that the initially

<sup>1</sup>National Oceanography Centre, University of Southampton, Southampton, UK.

<sup>2</sup>Institute of Geosciences, University of Tübingen, Tübingen, Germany.

<sup>3</sup>Lamont-Doherty Earth Observatory, Palisades, New York, USA.

proposed Antarctic-style timing of sea level variations [Siddall *et al.*, 2003; Rohling *et al.*, 2004] was in error. However, there are several complications that could preclude such a firm conclusion.

[5] First, there is considerable scope for bias in radiocarbon dating of Red Sea material (notably in older, MIS 3, intervals where residual  $^{14}\text{C}$  concentrations are low). This is because of aragonite precipitation, especially in high-salinity low sea level intervals, and/or because of early diagenetic precipitation of secondary (high Mg) calcite. While these phases can be easily removed when preparing small quantities of foraminiferal calcite for stable isotope analyses, they are impossible to avoid when picking the large quantities of material needed for radiocarbon dating, and even small amounts of secondary material will have significant impact on datings of foraminiferal calcite in intervals with low residual  $^{14}\text{C}$  activity. This introduces potential bias into radiocarbon dating, especially in glacial intervals, even in cases with perfect stratigraphy.

[6] In addition, the reservoir age of water in the Red Sea becomes greatly enhanced with sea level lowering (which is the crux of the Red Sea sea level method [Rohling *et al.*, 1998; Siddall *et al.*, 2003, 2004]). Hence, considerable variation can be expected through time in the reservoir age correction that should be applied to Red Sea marine radiocarbon datings. The exchange fluxes through Bab-el-Mandab reported by Sofianos *et al.* [2002] and Siddall *et al.* [2002] imply present-day residence times for water in the Red Sea of about 20 years (basin-averaged value) and about 300 years (deep waters, based on the estimate of Eshel *et al.* [1994] for the aspired deep water flux over the sill). For a glacial sea level lowstand of  $-120$  m, the exchange fluxes calculated by Siddall *et al.* [2004] would imply increases in these values up to 180 years (basin-averaged) and 2200 years (deep waters), and for MIS 3 sea level stands of  $-60$  to  $-90$  m, these values would be 25 to 40, and 300 to 500 years, respectively. The calculated maximum for glacial maximum conditions likely is an overestimate, given that oxygen-dependent benthic foraminifera continued to live in the deep basin [e.g., Rohling *et al.*, 1998; Fenton *et al.*, 2000], and that there was active deep water formation in the northern Red Sea during glacial times [Arz *et al.*, 2003]. It nevertheless remains evident that even the residence times of water increase considerably with lowering of sea level, and residence times of carbon in the basin would be affected by at least similar values. Stratification influences also come into play, especially where carbon exchange is concerned. Particularly pronounced residence time contrasts may develop between water masses at times of rising sea level, when salinity decrease in the basin reduces the potential for newly formed deep water to displace existing, highly saline deep waters (see Rohling [1994] for elaboration of a Mediterranean analog). Arz *et al.* [2003] argue that water column stratification and consequent “isolation” of deep waters contributed to the deposition of organic-rich sediments in the Red Sea during deglaciations. In view of the variable, sea level-dependent residence times of water within the Red Sea, it may be expected that radiocarbon reservoir age corrections varied with sea level as well. The outlined problems with radiocarbon dating in Red Sea

records imply that, although a reasonable rough chronology might be developed for the last 40,000 years using AMS  $^{14}\text{C}$  datings, such a framework will be insufficiently constrained to reveal details about millennial-scale phase relationships relative to other paleoclimate archives.

[7] Finally, to extend their radiocarbon-based Red Sea chronology beyond 40 cal ka BP, Arz *et al.* [2007] used 3 paleointensity tie points to constrain the chronology between 65 and 41 ka. Such a small number of age tie points for this 24 ka age interval precludes establishment of a chronology with the centennial- to millennial-scale resolution required to synchronize sea level variability with the Greenland ice cores, especially if the record contains variations in sedimentation rate [cf. Roberts and Winkhofer, 2004]. Moreover, uncertainty concerning the lock-in depth of a postdepositional remanent magnetization reduces confidence in the direct pinning by Arz *et al.* [2007] of a sea level event to the Laschamp event, because the magnetization and the event to which it is stratigraphically linked are not necessarily synchronous [Roberts and Winkhofer, 2004]. Synchronization with much smaller age uncertainties is required before the phasing of sea level variability can be established relative to the Greenland ice cores within this key interval.

## 2. Relative Timing and Phase Relationships

[8] The most conclusive way of establishing centennial- to millennial-scale phase relationships between paleoclimate archives is through use of coregistered signals [e.g., Blunier *et al.*, 1998; Shackleton *et al.*, 2000; Rohling and Pälike, 2005]. Using variations in concentration of atmospherically well-mixed methane gas in air bubbles trapped in ice, Blunier *et al.* [1998], Blunier and Brook [2001], and EPICA Community Members [2006] established the phase relationship between Greenland (Dansgaard-Oeschger; DO-style) climate variability, and Antarctic-style climate variability. The phase relationship between climate variability in the two polar regions as inferred from methane synchronization has been independently corroborated by Shackleton *et al.* [2000]. Those authors found that planktonic foraminiferal  $\delta^{18}\text{O}$  in core MD95–2042 from the Iberian margin (eastern North Atlantic) has strong signal similarity with DO-style variability, while deep water variations (3140 m water depth) recorded by  $\delta^{18}\text{O}$  in benthic foraminifera from the same samples show a clear Antarctic-style signature.

[9] Here we employ coregistered records to evaluate the phasing of the Red Sea stable oxygen isotope (sea level proxy) record relative to the methane-synchronized Antarctic and Greenland paleotemperature proxy records. We use two independent parameters from a single central Red Sea sediment core (GeoTü-KL11) through MIS 3 [Hemleben *et al.*, 1996; Siddall *et al.*, 2003], namely stable oxygen isotope ratios in the surface-dwelling planktonic foraminiferal species *Globigerinoides ruber* (white) ( $\delta^{18}\text{O}_{\text{ruber}}$ ) and bulk sediment magnetic susceptibility. Both were measured on a continuous series of 1-cm spaced samples.

[10] The  $\delta^{18}\text{O}_{\text{ruber}}$  series underlies the sea level reconstructions from the Red Sea method [Siddall *et al.*, 2003]. Magnetic susceptibility can sometimes provide a proxy for

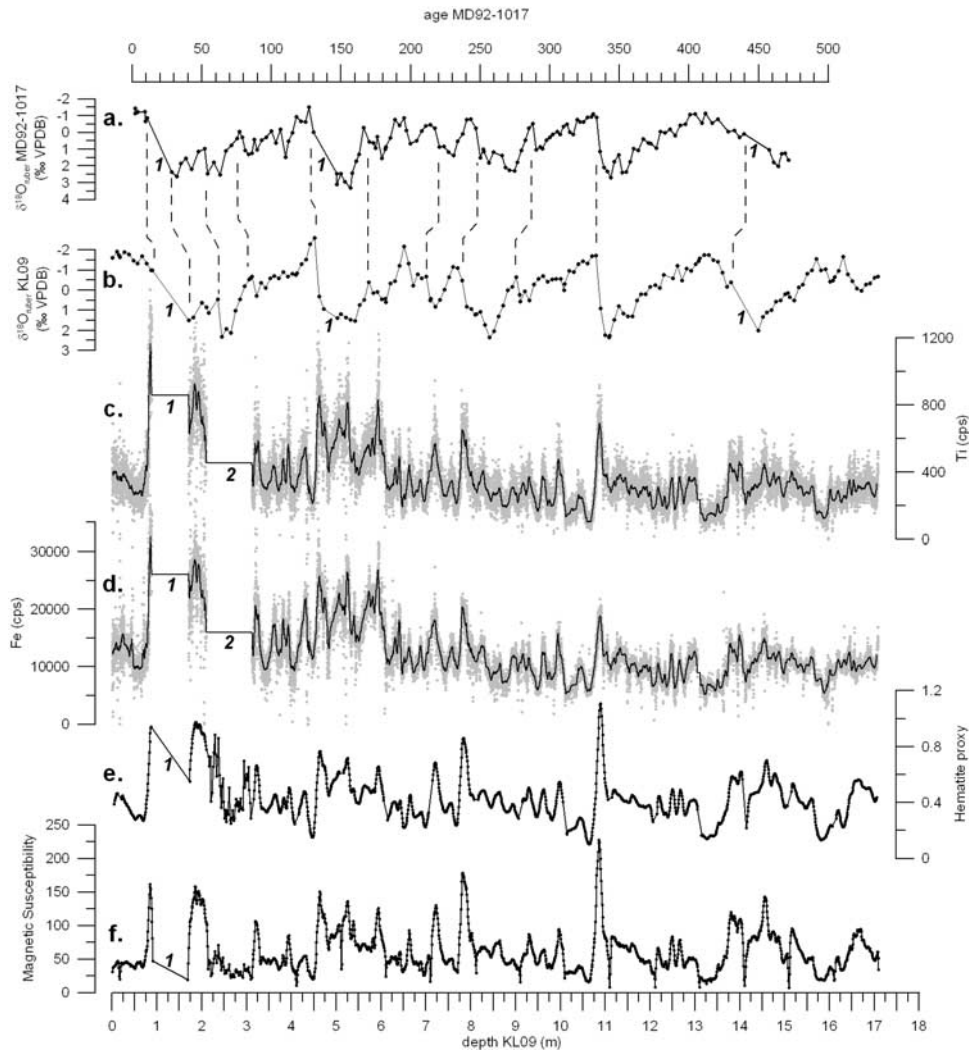


**Figure 1.** Records for central Red Sea core GeoTü-KL09 ( $19^{\circ}57.6'N$ ,  $38^{\circ}08.3'E$ , 814 m water depth). Number 1 indicates gap in records due to the presence of indurated aplanktonic zones (see *Fenton et al.* [2000] for discussion), and number 2 indicates lack of data because of relatively dry sediment surface that could not be sampled with U channels and so could not be analyzed with the core scanner XRF. Through the interval labeled 2, magnetic properties were analyzed using a continuous series of discrete  $2 \times 2 \times 2$  cm “cube” samples. (a) Chronology based on stable oxygen isotope stratigraphy of the previous longest Red Sea record, from central Red Sea core MD92-1017 [*Rohling et al.*, 1998; *Fenton et al.*, 2000]. (b) Stable oxygen isotope record for core KL09 versus depth in core (bottom axis) with (dashed) tie lines to the chronology of MD92-1017. (c) ITRAX core scanner XRF Ti counts in KL09 at 0.5 mm resolution, with 4 cm moving average filter to obtain a resolution that is visually similar to that of the whole-core environmental magnetic analyses, where the magnetometer response function imposes a  $\sim 4$  cm moving Gaussian filtering. (d) ITRAX core scanner XRF Fe counts in KL09, with same filtering as in Figure 1c. (e) Environmental magnetic hematite proxy record [after *Larrasoana et al.*, 2003, 2008]. (f) Magnetic susceptibility record for core KL09.

colian dust content in sediments. In this case, it is a measure of variability in the regional (wider Arabian Sea) monsoon climate, which was found to have followed the Greenland DO-style rhythm [*Schulz et al.*, 1998; *Leuschner and Sirocko*, 2000; *Burns et al.*, 2003; *Rohling et al.*, 2003]. However, the use of magnetic susceptibility as a proxy for eolian dust is warranted only when this relationship is confirmed by comparison with independent indicators of eolian dust concentration [e.g., *Larrasoana et al.*, 2003,

2008]. We therefore first establish the extent to which central Red Sea magnetic susceptibility represents eolian dust content, by comparing magnetic measurements and core-scanning X-ray fluorescence (XRF) results for nearby core GeoTü-KL09, which was freshly opened and sampled with u channels (October 2005) to measure signals unaffected by any potential alterations. Such whole-core (u channel) sampling was no longer possible in KL11, as this core is stored in a dry condition, but we were able to



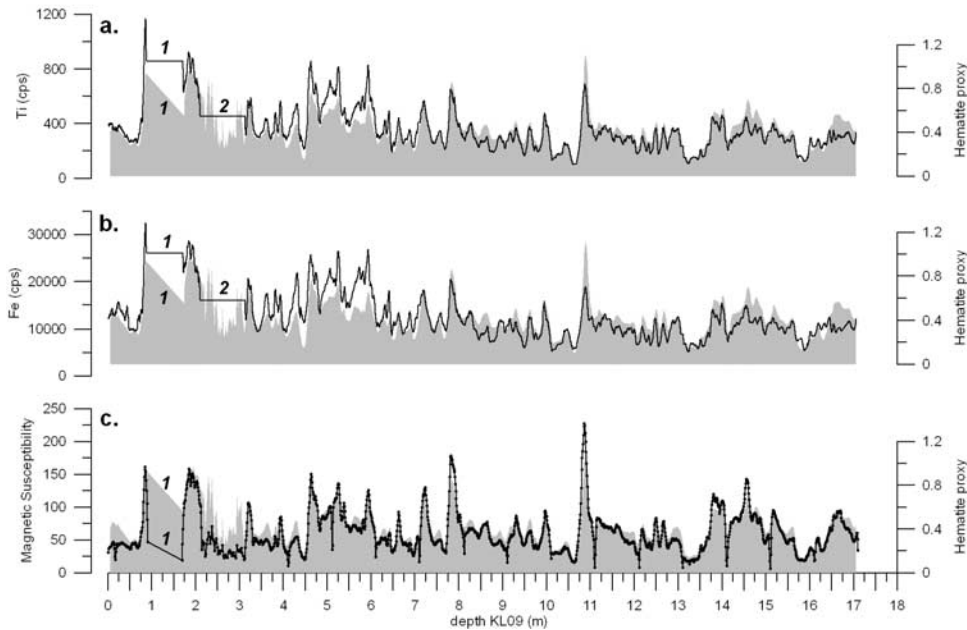


**Figure 2.** Superimposed plots for sediment core KL09 of (a) environmental magnetic hematite proxy (gray) and the filtered XRF-based Ti record (black) and (b) environmental magnetic hematite proxy (gray) and the filtered XRF-based Fe record (black). These plots demonstrate a close structural similarity in fluctuations of the hematite proxy and those of geochemical indicators of eolian dust content (as also found by *Larrasoña et al.* [2003] in the eastern Mediterranean Sea). (c) Superimposed magnetic susceptibility record (black) with the hematite proxy record (gray), which again reveals strong structural similarity (see also Figure 3).

carefully remove a continuous series of 1-cm spaced discrete samples.

### 3. Results and Discussion

[11] In Figure 1, we show for core KL09 the elemental counts of Fe and Ti from an ITRAX core-scanning XRF system (0.5 mm increments) and an environmental magnetic proxy for hematite concentration determined using a 2-G Enterprises cryogenic magnetometer ( $IRM_{0.9 T@AF120 mT}$ , after *Larrasoña et al.* [2003]). These records are presented alongside a low-resolution  $\delta^{18}O_{\text{ruber}}$  record from a Geo2020 mass spectrometer with individual acid bath preparation line (Figure 1). A working chronology was obtained for KL09 by visually correlating the latter with  $\delta^{18}O_{\text{ruber}}$  data from core MD92–1017, the published central Red Sea record with the longest time coverage [*Rohling et al.*, 1998; *Siddall et al.*, 2003].

[12] Figure 2 compares our hematite proxy record with Fe and Ti abundance data, which have previously been found to provide sound indicators of eolian dust fluctuations in the region [*Ivanochko et al.*, 2005]. Variability in the hematite proxy record shows strong similarity with that in the smoothed Fe series (4 cm moving average to approximate the smoothing effect of the magnetometer’s response coil width), which indicates that variability in Fe content is predominantly associated with hematite fluctuations (Figure 2b). The hematite proxy is strongly similar to the Ti record (Figure 2a), a much used proxy for eolian dust

throughout the Mediterranean/Middle East region [e.g., *Wehausen and Brumsack*, 2000; *Lourens et al.*, 2001; *Larrasoña et al.*, 2003; *Ivanochko et al.*, 2005]. We therefore conclude that the hematite proxy offers a good representation of eolian dust content in our central Red Sea sediments, similar to the eastern Mediterranean [*Larrasoña et al.*, 2003].

[13] The hematite proxy and magnetic susceptibility data collected on the same samples have similar variability (Figure 2c). In quantitative terms, these series share 81% common variance, where  $N = 1447$ , although the nonzero intercept in Figure 3 indicates some background magnetic susceptibility that is carried by minerals other than hematite. Nevertheless, it is evident that magnetic susceptibility fluctuations in central Red Sea sediments provide a useful proxy for eolian dust variations. This is advantageous, because magnetic susceptibility is easy to measure on small, discrete samples in a continuous series of narrow depth increments, which allows development of highly resolved eolian dust proxy records for the central Red Sea.

[14] We measured the magnetic susceptibility of small, dried, discrete, 1-cm samples from core KL11, to allow comparison of the resultant high-resolution eolian dust proxy record with the previously published  $\delta^{18}O_{\text{ruber}}$  (sea level proxy) series for the same samples [*Siddall et al.*, 2003]. The complete data set is presented in auxiliary material for the entire 70–23 ka BP interval analyzed.<sup>1</sup>

<sup>1</sup>Auxiliary materials are available at <ftp://ftp.agu.org/apend/pa/2008pa001617>.

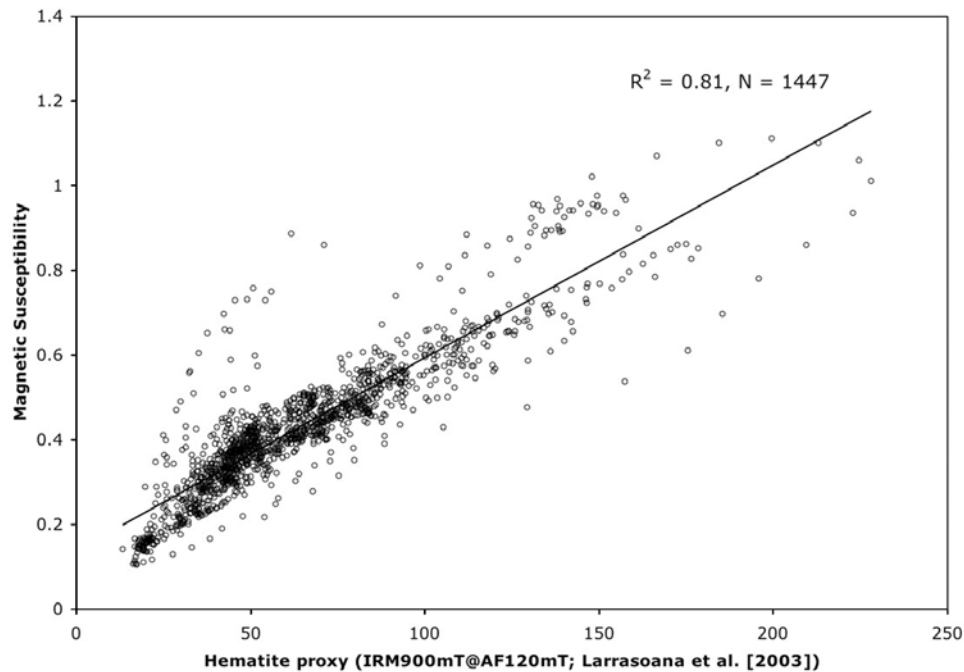


**Figure 3.** Regression plot of the magnetic susceptibility versus hematite proxy data in core KL09. This demonstrates a strong correlation ( $R^2 = 0.81$  for  $N = 1447$ ), which indicates that magnetic susceptibility suitably reflects hematite concentrations (eolian dust) in central Red Sea sediments.

Here we focus on the 64–36 ka BP interval because this is where the contended millennial-scale sea level fluctuations are found [Siddall *et al.*, 2003; Rohling *et al.*, 2004], while we note also that magnetic susceptibility in younger levels appears to lose millennial-scale definition. Comparable loss of millennial-scale definition from about 36 ka BP into the Last Glacial Maximum can be seen in high-resolution eolian proxy data from core 905, recovered just outside the Gulf of Aden in the SW Arabian Sea [Ivanochko *et al.*, 2005].

[15] The coregistered  $\delta^{18}\text{O}_{\text{ruber}}$  (sea level proxy) and magnetic susceptibility (eolian dust proxy) records clearly fluctuate out of phase within early and middle MIS 3 (Figure 4c, and refer to the auxiliary material for offsets in terms of depth). As in the studies of Siddall *et al.* [2003, 2008b] and Rohling *et al.* [2004], we synchronize (“tune”) the  $\delta^{18}\text{O}_{\text{ruber}}$  (sea level proxy) series to the Antarctic  $\delta^{18}\text{O}_{\text{ice}}$  series from Byrd station, which because of methane synchronization between Byrd and GISP2 [Blunier *et al.*, 1998; Blunier and Brook, 2001] places the Red Sea records on a (GISP2) time scale that allows direct comparison with both ice core records. We find that this tuning (see tie points in Figure 4a) not only produces an excellent fit between the Red Sea  $\delta^{18}\text{O}_{\text{ruber}}$  (sea level proxy) series and the Byrd  $\delta^{18}\text{O}_{\text{ice}}$  series (Figure 4a), but that it also results in a coherent phasing of the major shifts in the coregistered eolian dust record with the Greenland  $\delta^{18}\text{O}_{\text{ice}}$  series (Figure 4d).

[16] The coregistered Red Sea records presented here provide important insights into the sensitivity of the various proxies from this basin. It has been documented that Arabian Sea monsoon variations during MIS 3 closely followed DO-style variations (Figures 4d and 4e) [e.g., Schulz *et al.*, 1998; Ivanochko *et al.*, 2005]. Hence, regional climate variability over the Red Sea may be expected to

follow this rhythm as well. Eolian dust fluxes into the central Red Sea appear to have fluctuated in compliance with this expectation (Figure 4e).

[17] The surface-dwelling planktonic foraminifer *Globigerinoides ruber* gives a Red Sea  $\delta^{18}\text{O}_{\text{ruber}}$  record that markedly deviates from the a priori expectation of DO-style variability (Figure 4). In addition, the  $\delta^{18}\text{O}_{\text{ruber}}$  record shows a much greater glacial-interglacial amplitude than anywhere in the open ocean (almost 4 times amplified). There must therefore be a mechanism that (1) is much more important for Red Sea  $\delta^{18}\text{O}$  than regional climate fluctuations, (2) caused a strongly amplified response, and (3) fluctuated on a different rhythm than the regional climate. The Red Sea sea level method specifically addressed this mechanism [Siddall *et al.*, 2003, 2004; Biton *et al.*, 2008], by quantifying the amplified response of Red Sea  $\delta^{18}\text{O}_{\text{water}}$  (and so  $\delta^{18}\text{O}_{\text{ruber}}$ ) to sea level lowering, on the basis of water residence time increases in the basin due to reduction of water mass exchange across the very shallow (137 m) Red Sea sill. A residence time increase causes prolonged exposure of the Red Sea waters to high evaporation, which drives a rapid increase in  $\delta^{18}\text{O}$  [Siddall *et al.*, 2003, 2004; Biton *et al.*, 2008]. The coregistered timing relationship between  $\delta^{18}\text{O}_{\text{ruber}}$  and regional climate (as indicated by eolian dust) reported here implies that the sea level fluctuations ( $\delta^{18}\text{O}_{\text{ruber}}$ ) followed an Antarctic-style rhythm during early to middle MIS 3, while the regional climate (eolian dust proxy) followed the DO-style variability that also characterized the Arabian Sea monsoon.

[18] We emphasize that there has been no attempt to “tune” the eolian dust signal to the Greenland  $\delta^{18}\text{O}_{\text{ice}}$  fluctuations, but that it simply “falls into place” when the coregistered  $\delta^{18}\text{O}_{\text{ruber}}$  (sea level) series is correlated with the

Antarctic Byrd  $\delta^{18}\text{O}_{\text{ice}}$  series. Thus, we independently diagnose that the eolian dust series seems to fluctuate through early to middle MIS 3 with a timing close to the main DO events in Greenland. While this corroborates previous suggestions that regional eolian dust fluxes show DO-style variability [e.g., *Ivanochko et al.*, 2005], our records for the first time provide evidence that does not include some degree of chronological tuning to the Greenland record.

#### 4. Summary and Implications

[19] Central Red Sea  $\delta^{18}\text{O}_{\text{ruber}}$  (sea level proxy) shares a remarkable signal structure with Antarctic-style temperature proxy records, and with deep-sea benthic foraminiferal  $\delta^{18}\text{O}$  records [*Siddall et al.*, 2003; *Rohling et al.*, 2004]. We find that the coregistered eolian dust record shares considerable signal similarity with Greenland DO-style variability, especially in early to middle MIS 3. Moreover, we observe that the offset timing relationship between the coregistered sea level and eolian dust records in the central Red Sea is

similar to that found with methane synchronization between Antarctic and Greenland climate records [*Blunier et al.*, 1998; *Blunier and Brook*, 2001; *EPICA Community Members*, 2006], and thus is also close to that between coregistered Antarctic-style  $\delta^{18}\text{O}_{\text{benthic}}$  and DO-style  $\delta^{18}\text{O}_{\text{planktonic}}$  on the Iberian margin [*Shackleton et al.*, 2000]. We conclude that the Red Sea  $\delta^{18}\text{O}_{\text{ruber}}$  (sea level proxy) series during early to middle MIS 3 follows an Antarctic-style timing, as was initially proposed [*Siddall et al.*, 2003; *Rohling et al.*, 2004]. We therefore reject the suggestion of *Arz et al.* [2007] that the sea level record is more closely related to DO-style variability.

[20] Although we assert that the sea level fluctuations followed an Antarctic-style timing, this does not imply that these fluctuations derived exclusively from Antarctic ice volume. Rather, a key component appears to have derived from northern ice sheets. For example, *Rohling et al.* [2004] suggest from the use of stable oxygen isotopes as a tracer in an Earth System model that the most realistic distribution simulations would require contributions from both hemispheres, *Hill et al.* [2006] report evidence for significant meltwater flux from the Southern Laurentide margin on an Antarctic-style timing, and *Clark et al.*'s [2007] comprehensive modeling results invoke large-scale waxing and waning of the Laurentide ice sheet on an Antarctic-style rhythm.

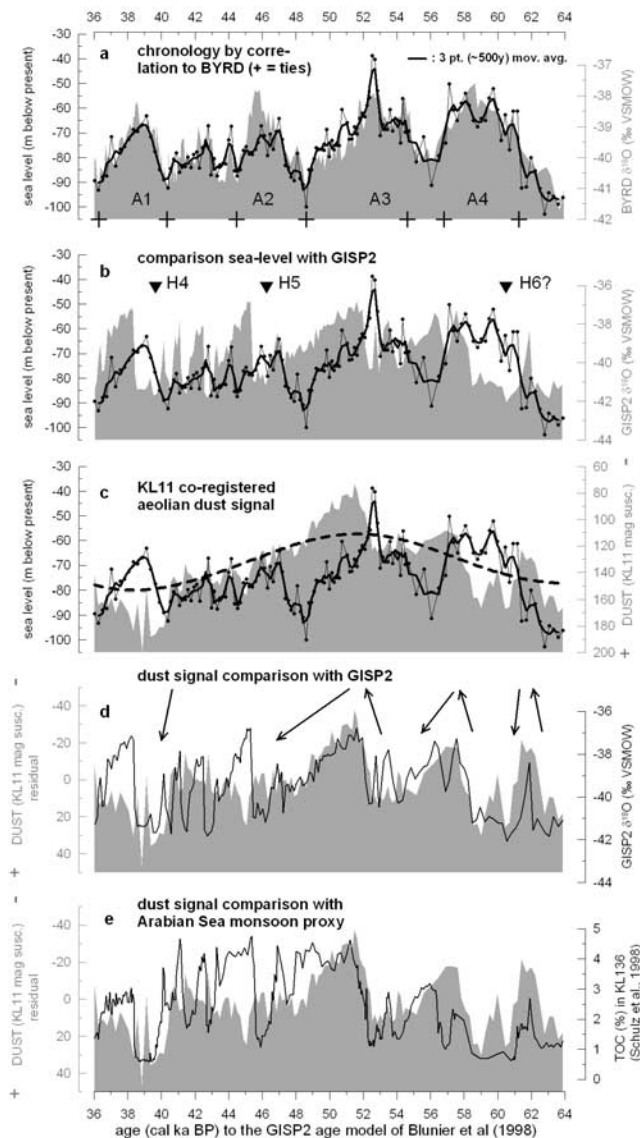


**Figure 4.** (a and b) Sea level record from the *Siddall et al.* [2003] Red Sea method in core GeoTü-KL11 ( $18^{\circ}44.5'N$ ,  $39^{\circ}20.6'E$ , 825 m water depth) (dots, thin line), with 500 year moving average (heavy line), after *Rohling et al.* [2004]. The gray shaded record in Figure 4a is the Antarctic ice- $\delta^{18}\text{O}$  temperature proxy record from Byrd ice core, methane synchronized to the GISP2 time scale [after *Blunier et al.*, 1998], and Antarctic warm events are indicated with conventional “A” numbers. Crosses indicate chronostratigraphic tie points. Grey shaded record in Figure 4b is the Greenland GISP2 ice- $\delta^{18}\text{O}$  temperature proxy record on the time scale used in the Antarctic-Greenland synchronizations of *Blunier et al.* [1998] and as used also for the Red Sea sea level record given by *Siddall et al.* [2003] and *Rohling et al.* [2004]. Heinrich events are indicated with conventional “H” numbers. Note that the present paper is not primarily concerned with absolute age but focuses on comparisons of the Red Sea records with the relative timing relationship between Greenland and Antarctic  $\delta^{18}\text{O}$  records. (c) Sea level data together with (gray shaded) magnetic susceptibility (windblown dust) data from the same sample series of KL11. The dashed line indicates a longer-term trend in the dust data. (d) Comparison of magnetic susceptibility (eolian dust) data for KL11 after removal of the longer-term trend (gray shaded) with the Greenland GISP2 ice- $\delta^{18}\text{O}$  record. There is good agreement in the timing of major transitions (arrows) between these two records. (e) Comparison between magnetic susceptibility (eolian dust) data for KL11 after removal of the longer-term trend (gray shaded) with the Arabian Sea total organic carbon record of *Schulz et al.* [1998], which established for the first time that regional Arabian Sea climate changed on timings similar to the Greenland climate record.



[21] Our results strongly confirm that early to middle MIS 3 sea level rises, indicated by shifts in Red Sea  $\delta^{18}\text{O}_{\text{ruber}}$  to lighter values, occurred during cold episodes in Greenland. Because regional Arabian Sea climate was found to have fluctuated close to the Greenland DO rhythm [e.g., Schulz *et al.*, 1998; Ivanochko *et al.*, 2005], this implies that shifts of Red Sea  $\delta^{18}\text{O}_{\text{ruber}}$  to lighter values coincided with cooler and more arid regional climate conditions (in agreement with our enhanced eolian dust fluxes). Such a regional climatic imprint would tend to have driven  $\delta^{18}\text{O}_{\text{ruber}}$  in the opposite sense to that observed. It is therefore unlikely that the amplitudes of MIS 3 sea level changes obtained from Red Sea records would be overestimated because of any overlooked regional temperature and aridity effects. Instead, the present study's information on the likely phasing of such effects would imply that their detailed inclusion in the sea level reconstructions may push the amplitude estimates toward the high end of the reported uncertainty intervals [Siddall *et al.*, 2003; Rohling *et al.*, 2004].

[22] Finally, we comment on the potential influence of any isostatic effects. Initial estimates for isostatic effects reach up to 17 m at Bab-el-Mandab over a full glacial-interglacial range [Siddall *et al.*, 2004; Biton *et al.*, 2008].

If we generously assume that the isostatic effects reached full steady state during the rapid MIS 3 sea level fluctuations, and that they scale in a roughly linear manner with sea level change (the latter produces an overestimate of isostatic effects because virtually all of the roughly 50 m deep Red Sea shelf area would continuously be above sea level during MIS 3), then isostatic effects in the sea level range of MIS 3 (−60 to −90 m) would at most vary between 8.5 and 12.8 m. Therefore, isostatic effects cannot explain more than  $12.8 - 8.5 = 4.3$  m of the sea level variability recorded in MIS 3 by the Red Sea method.

[23] Overall, our analysis offers strong support for the earlier conclusions of Siddall *et al.* [2003], that the sea level variations during early to middle MIS 3 were of large (order 25–30 m) amplitude, and followed a timing similar to Antarctic-style climate variations.

[24] **Acknowledgments.** This study contributes to UK Natural Environment Research Council (NERC) project NE/C003152/1, NERC consortium Response of humans to abrupt environmental transitions (RESET, NE/E01531X/1), and German Science Foundation (DFG) project He 697/17; Ku 2259/3. Mark Siddall is supported by an RCUK fellowship from the University of Bristol and by Lamont Doherty Earth Observatory.

## References

- Arz, H. W., J. Pätzold, P. J. Müller, and M. O. Moammar (2003), Influence of Northern Hemisphere climate and global sea level rise on the restricted Red Sea marine environment during termination I, *Paleoceanography*, 18(2), 1053, doi:10.1029/2002PA000864.
- Arz, H. W., F. Lamy, A. Ganopolski, N. Nowaczyk, and J. Pätzold (2007), Dominant Northern Hemisphere climate control over millennial-scale glacial sea-level variability, *Quat. Sci. Rev.*, 26, 312–321, doi:10.1016/j.quascirev.2006.07.016.
- Biton, E., H. Gildor, and W. R. Peltier (2008), Relative sea level reduction at the Red Sea during the Last Glacial Maximum, *Paleoceanography*, 23, PA1214, doi:10.1029/2007PA001431.
- Blunier, T., and E. Brook (2001), Timing of millennial-scale climate change in Antarctica and Greenland during the last glacial period, *Science*, 291, 109–112, doi:10.1126/science.291.5501.109.
- Blunier, T., *et al.* (1998), Asynchrony of Antarctica and Greenland climate during the last glacial, *Nature*, 394, 739–743, doi:10.1038/29447.
- Burns, S. J., D. Fleitmann, A. Matter, J. Kramers, and A. A. Al-Subbaray (2003), Indian Ocean climate and an absolute chronology over Dansgaard-Oeschger Events 9 to 13, *Science*, 301, 1365–1367, doi:10.1126/science.1086227.
- Clark, P. U., S. W. Hostetler, N. G. Pisias, A. Schmittner, and K. J. Meissner (2007), Mechanisms for a ~7-kyr climate and sea-level oscillation during marine isotope stage 3, in *Ocean Circulation: Mechanisms and Impacts*, *Geophys. Monogr. Ser.*, vol. 173, edited by A. Schmittner, J. Chiang, and S. Hemming, pp. 209–246, AGU, Washington, D. C.
- Cutler, K. B., R. L. Edwards, F. W. Taylor, H. Cheng, J. Adkins, C. D. Gallup, P. M. Cutler, G. S. Burr, and A. L. Bloom (2003), Rapid sea-level fall and deep-ocean temperature change since the last interglacial period, *Earth Planet. Sci. Lett.*, 206, 253–271, doi:10.1016/S0012-821X(02)01107-X.
- EPICA Community Members (2006), One-to-one interhemispheric coupling of polar climate variability during the last glacial, *Nature*, 444, 195–198, doi:10.1038/nature05301.
- Eshel, G., M. A. Cane, and M. B. Blumenthal (1994), Modes of subsurface, intermediate, and deep water renewal in the Red Sea, *J. Geophys. Res.*, 99, 15,941–15,952, doi:10.1029/94JC01131.
- Fenton, M., S. Geiselhart, E. J. Rohling, and C. Hemleben (2000), Aplanktonic zones in the Red Sea, *Mar. Micropaleontol.*, 40, 277–294, doi:10.1016/S0377-8398(00)00042-6.
- Hemleben, C., D. Meischner, R. Zahn, A. Almogilabini, H. Erlenkeuser, and B. Hiller (1996), Three hundred eighty thousand year long stable isotope and faunal records from the Red Sea: Influence of global sea level change on hydrography, *Paleoceanography*, 11, 147–156, doi:10.1029/95PA03838.
- Hill, H. W., B. P. Flower, T. M. Quinn, D. J. Hollander, and T. P. Guilderson (2006), Laurentide Ice Sheet meltwater and abrupt climate change during the last glaciation, *Paleoceanography*, 21, PA1006, doi:10.1029/2005PA001186.
- Ivanochko, T. S., R. S. Ganeshram, G. J. A. Brummer, G. Ganssen, S. J. A. Jung, S. G. Moreton, and D. Kroon (2005), Variations in tropical convection as an amplifier of global climate change at the millennial scale, *Earth Planet. Sci. Lett.*, 235, 302–314, doi:10.1016/j.epsl.2005.04.002.
- Larrasoana, J., A. P. Roberts, E. J. Rohling, M. Winkhofer, and R. Wehausen (2003), Three million years of monsoon variability over the northern Sahara, *Clim. Dyn.*, 21, 689–698, doi:10.1007/s00382-003-0355-z.
- Larrasoana, J., A. P. Roberts, and E. J. Rohling (2008), Magnetic susceptibility of Mediterranean marine sediments as a proxy for Saharan dust supply?, *Mar. Geol.*, 254, 224–229, doi:10.1016/j.margeo.2008.06.003.
- Leuschner, D. C., and F. Sirocko (2000), The low-latitude monsoon climate during Dansgaard-Oeschger cycles and Heinrich events, *Quat. Sci. Rev.*, 19, 243–254, doi:10.1016/S0277-3791(99)00064-5.
- Lisiecki, L. E., and M. E. Raymo (2005), A Pliocene-Pleistocene stack of 57 globally distributed benthic delta O-18 records, *Paleoceanography*, 20, PA1003, doi:10.1029/2004PA001071.
- Lourens, L. J., R. Wehausen, and H.-J. Brumsack (2001), Geological constraints on tidal dissipation and dynamical ellipticity of the Earth over the past three million years, *Nature*, 409, 1029–1033, doi:10.1038/35059062.
- Muscheler, R., J. Beer, P. W. Kubik, and H.-A. Synal (2005), Geomagnetic field intensity during the last 6000 years based on  $^{10}\text{Be}$  and  $^{36}\text{Cl}$  from the summit ice cores and  $^{14}\text{C}$ , *Quat. Sci. Rev.*, 24, 1849–1860, doi:10.1016/j.quascirev.2005.01.012.
- Pahnke, K., and R. Zahn (2005), Southern hemisphere water mass conversion linked with North Atlantic climate variability, *Science*, 307, 1741–1746, doi:10.1126/science.1102163.
- Pahnke, K., R. Zahn, H. Elderfield, and M. Schulz (2003), 340,000-year centennial-scale marine record of Southern Hemisphere climatic oscillation, *Science*, 301, 948–952, doi:10.1126/science.1084451.
- Roberts, A. P., and M. Winkhofer (2004), Why are geomagnetic excursions not always recorded in sediments? Constraints from post-depositional remanent magnetization lock-in modelling, *Earth Planet. Sci. Lett.*, 227, 345–359, doi:10.1016/j.epsl.2004.07.040.
- Rohling, E. J. (1994), Review and new aspects concerning the formation of Mediterranean sapropels, *Mar. Geol.*, 122, 1–28, doi:10.1016/0025-3227(94)90202-X.
- Rohling, E. J., and H. Pälike (2005), Centennial-scale climate cooling with a sudden cold event

- around 8,200 years ago, *Nature*, 434, 975–979, doi:10.1038/nature03421.
- Rohling, E. J., M. Fenton, F. J. Jorissen, P. Bertrand, G. Ganssen, and J. P. Caulet (1998), Magnitudes of sea-level lowstands of the past 500000 years, *Nature*, 394, 162–165, doi:10.1038/28134.
- Rohling, E. J., P. A. Mayewski, and P. Challenor (2003), On the timing and mechanism of millennial-scale climate variability during the last glacial cycle, *Clim. Dyn.*, 20, 257–267.
- Rohling, E. J., R. Marsh, N. C. Wells, M. Siddall, and N. R. Edwards (2004), Similar meltwater contributions to glacial sea level changes from Antarctic and northern ice sheets, *Nature*, 430, 1016–1021, doi:10.1038/nature02859.
- Schulz, H., U. von Rad, and H. Erlenkeuser (1998), Correlation between Arabian Sea and Greenland climate oscillations of the past 110,000 years, *Nature*, 393, 54–57.
- Shackleton, N. J., M. A. Hall, and E. Vincent (2000), Phase relationships between millennial-scale events 64,000–24,000 years ago, *Paleoceanography*, 15, 565–569, doi:10.1029/2000PA000513.
- Siddall, M., D. Smeed, S. Mathiessen, and E. J. Rohling (2002), Modelling the seasonal cycle of the exchange flow in Bab-el-Mandab (Red Sea), *Deep Sea Res. Part I*, 49, 1551–1569, doi:10.1016/S0967-0637(02)00043-2.
- Siddall, M., E. J. Rohling, A. Almogi-Labin, C. Hemleben, D. Meischner, I. Schmelzer, and D. A. Smeed (2003), Sea-level fluctuations during the last glacial cycle, *Nature*, 423, 853–858, doi:10.1038/nature01690.
- Siddall, M., D. A. Smeed, C. Hemleben, E. J. Rohling, I. Schmelzer, and W. R. Peltier (2004), Understanding the Red Sea response to sea level, *Earth Planet. Sci. Lett.*, 225, 421–434, doi:10.1016/j.epsl.2004.06.008.
- Siddall, M., E. J. Rohling, and H. W. Arz (2008a), Convincing evidence for rapid ice sheet growth during the last glacial period, *PAGES News*, 16(1), 15–16.
- Siddall, M., E. J. Rohling, W. G. Thompson, and C. Waelbroeck (2008b), MIS 3 sea-level changes: Data synthesis and new outlook, *Rev. Geophys.*, doi:10.1029/2007RG000226, in press.
- Sofianos, S. S., W. Johns, and S. P. Murray (2002), Heat and freshwater budgets in the Red Sea from direct observations at Bab-el-Mandab, *Deep Sea Res. Part II*, 49, 1323–1340, doi:10.1016/S0967-0645(01)00164-3.
- Wehausen, R., and H.-J. Brumsack (2000), Chemical cycles in Pliocene sapropel-bearing and sapropel-barren eastern Mediterranean sediments, *Palaeogeogr. Palaeoclimatol. Palaeoecol.*, 158, 325–352, doi:10.1016/S0031-0182(00)00057-2.

---

K. Grant, A. P. Roberts, and E. J. Rohling, National Oceanography Centre, University of Southampton, Southampton SO14 3ZH, UK. (e.rohling@noc.soton.ac.uk)

C. Hemleben, M. Kucera, I. Schmelzer, H. Schulz, M. Siccha, and G. Trommer, Institute of Geosciences, University of Tübingen, Sigwartstrasse 10, D-72076, Tübingen, Germany.

M. Siddall, Lamont-Doherty Earth Observatory, 61 Route 9W, P.O. Box 1000, Palisades, NY 10964-8000, USA.